Word count: 8712

A scalable life cycle assessment for alternating and direct current microgrids for office buildings

Christina Kockel[1,4*], Lars Nolting[1,4], Rafael Goldbeck[2,4], Christina Wulf[3,5], Rik W. De Doncker[2,4], Aaron Praktiknjo[1,4*]

[1] Institute for Future Energy Consumer Needs and Behavior, RWTH Aachen University, 52074 Aachen, Germany
[2] Institute for Power Electronics and Electrical Drives, RWTH Aachen University, 52066 Aachen, Germany
[3] Institute of Energy and Climate Research–Systems Analysis and Technology Evaluation, Forschungszentrum Jülich, 52428 Jülich, Germany
[4] JARA-ENERGY, 52074 Aachen, Germany
[5] JARA-ENERGY, 52425 Jülich, Germany
*Corresponding author, E-mail Address: christina.kockel@eonerc.rwth-aachen.de, apraktiknjo@eonerc.rwth-aachen.de

Abstract

Microgrids integrating local renewable energy sources at low-voltage level show promising potentials in realizing a reliable, efficient, and clean supply of electricity. Further improvements are expected when such a microgrid is operated on direct current (dc) instead of alternating current (ac) infrastructure for power distribution commonly in use today. Our study aims to systemically quantify the gap between environmental impacts of microgrids at building level using the case study of power distribution within office buildings. For this purpose, a scalable comparative life cycle assessment (LCA) is conducted based on a technical bottom-up analysis of differences between ac and dc microgrids. Particularly, our approach combines the assessment of required power electronic components on a micro-level with the macro-level requirements for daily operation derived from a generic grid model. The results indicate that the environmental impacts of employed power electronics are substantially reduced by operating a microgrid based on dc power distribution infrastructure. Our sensitivity analyses show that efficient dc microgrids particularly lead to savings in climate change impact emissions. In addition, our study shows that the scaling of power electronics as it is currently state of the art in LCAs leads to inaccurate results. Therefore, our developed method applies a more technical approach, which enables a detailed analysis of the environmental impacts of power electronic components at system level. Thus, it lays the foundation for an evaluation criterion for a comprehensive assessment of technological changes within the framework of energy policy objectives.

Highlights:

- Methodology for scalable LCA to compare ac and dc distribution systems
- Substantial reduction in material usage through shift from ac to dc microgrids
- DC microgrid system with reduced emissions for almost all observed cases
- Energy mix identified as the main driver for climate change impact

Keywords: building energy demand, life cycle assessment, microgrid, direct current, resource efficiency

Nomenclature

Abbreviations

ac	Alternating current	PCC	Point of common coupling
DAB	Dual active bridge	PC	Personal computer
dc	Direct current	PCB	Printed circuit board
IGBT	Insulated gate bipolar transistors	PV	Photovoltaic
LCA	Life cycle assessment	t CO_2 eq	Ton carbon dioxide equivalent
LCIA	Life cycle inventory analysis	VSI	Voltage source inverter
LED	Light-emitting diodes		

Symbols

A	Area	h_{fl}	full load hours
E_{dem}	Demanded energy	η_i	Efficiency of power converter for device i
E_{gen}	Generated energy	i	Device
E_{PCC}	Balancing energy from public grid	j	Office type
f_{PV_util}	Utilization factor for PV system	M	Mass
g_i	Simultaneity factor	n_{ws}	Number of workstations
η_{acdc}	Efficiency between an ac and dc System	P	Power
		U	Voltage
η_{dist}	Efficiency of distribution	V	Volume

1. Introduction

To mitigate climate change, increasing shares of renewable energy are being integrated into energy systems. However, conventional grid structures are challenging the progress of the transition possibly requiring concepts which are less centralized regarding power transmission. In this regard, microgrids with integrated renewable generation seem promising in terms of reliability, efficiency, and sustainability. Current research indicates that the efficiency of such microgrids could be increased even further when applying grid structures that are operated on direct current (dc) instead of alternating current (ac) [1,2]. This is mainly due to the fact that many renewable energy sources and storage systems, as well as most loads, inherently require dc power. Additionally, modern motor loads and energy sources generating ac power are usually interfaced by a variable-speed drive, consisting of an ac-dc rectifier, a dc-dc converter, and a dc-ac inverter, to decouple the controllable rotor frequency from the fixed grid frequency. For dc microgrids, the inverter at the power electronic grid interface is obsolete for all loads and decentralized energy sources and therefore, fewer conversion steps and components are required. However, an additional converter stage at the so-called point of common coupling (PCC) is necessary to establish a connection to the existing public ac grid. Figure 1 exemplarily depicts the differences in power electronics between an ac and a dc microgrid in a building. A paradigm shift from ac to dc distribution grids at consumer- or building-level may contribute to more efficient use of the generated electrical energy in a progressively decentralized power supply system.

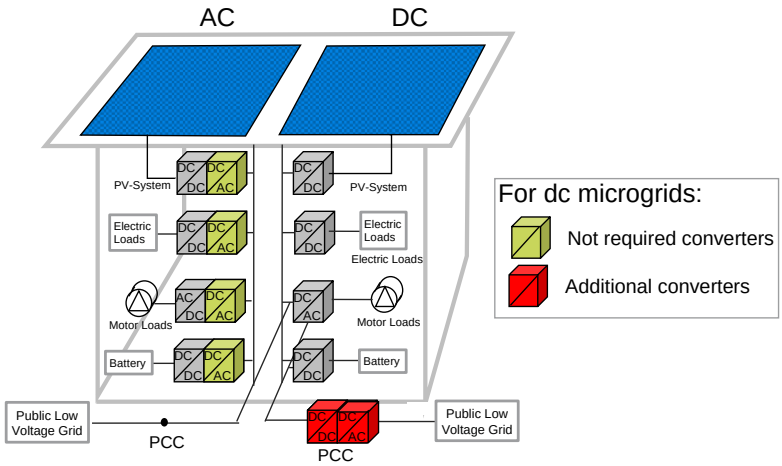

Figure 1: *Differences between ac and dc microgrids for a building grid based on De Doncker [3]*

However, environmental impacts of such a shift from ac to dc grids remain yet to be quantified. The consideration of this assessment dimension is particularly relevant against the background of the targeted reduction of greenhouse gas emissions and also the simultaneous objective of avoiding a shift of environmental impacts.

So far, some studies have assessed the environmental impact of microgrids in general by using the life cycle assessment (LCA) methodology. However, in these studies power electronics and converters have been considered rudimentarily, only. Even though they are mostly mentioned as important components of microgrids, they are either not considered in the assessment (see e.g. Wang et al. [4] and Das et al. [5]) or the material compositions are lacking levels of detail. In those cases, existing data sets for converters are utilized without specifying application, topology, and voltage class (e.g., in Smith et al. [6]) or the whole data sets are discretely scaled based on their weight and power levels to achieve the required performances, as exemplary shown by Papgeorigiou et al. [7]. However, in order to analyze the environmental impact of a transition to new dc-based grids, it is precisely these differences in topology and different voltage classes that are relevant. It also shows that a simple scaling of the mass proportional to the power class does not correspond to the reality of the design of converters. A more detailed study on the comparison of environmental impacts of dc and ac based systems and the utilized power electronics has been carried out by Kabus et al. [8]. However, their work focuses on charging infrastructures and cannot be directly transferred to different technological requirements as it is the case for microgrids. Nordelöf [9] presents a first approach for a scalable life cycle inventory depending on the voltage and power requirements of the inverter. Nonetheless, the analysis is specific for the power train of an electric vehicle and does not include a methodical scaling for all relevant power electronic components.

Our manuscript aims at filling this knowledge gap using an interdisciplinary approach and answering the research question: “What are the environmental impacts of ac and dc microgrids?” Our contribution to closing the research gap is threefold: (1) Assessing and comparing the environmental impacts of dc and ac based microgrids, (2) identifying the main drivers for emissions, and (3) enhancing the methodological basis for LCA of power electronics by adding a scalable approach. For this, we apply methods from the following research areas: power electronics and electricity distribution systems, LCA, and energy system analysis.

For our work, we chose to model the course of an entire life cycle of microgrids in scalable office buildings as case study. Office buildings represent a promising use case for the deployment of the new dc grid infrastructure. With large roof and façade areas in exposed locations, they are predestined for using photovoltaic (PV) systems. With similar electrical devices in every office and regulated working hours, they exhibit more homogeneous load profiles and allow for a better match between the load curve and the solar feed-in from the PV systems than most other types of buildings.

The remainder of our manuscript is structured as follows: In section 2, we briefly present theoretical background and state of research on the intersection between power electronics, system analysis, and LCA. We describe our methodology of combining the generic grid model with our comparative LCA in section 3. In section 4, we present our results of the analysis, before discussing them in section 5. Section 6 concludes our manuscript.

2. Theoretical background and state of research

Since the “war of currents” between Thomas Edison and George Westinghouse in the late 1800s, ac and dc technologies have been competing for the utilization in electricity supply. At that time, ac technology

was able to become the status quo technology due to less losses during power transmission and with this a centralized power supply system with large generation sides that utilize primarily fossil fuels was established [10]. In the course of the ongoing energy transition, the number of renewable generation units that are integrated into the electricity infrastructure at medium or low voltage levels is increasing [11]. This gradual change increasingly puts stress on the present ac-based power distribution system, causing struggles with voltage rises and protection issues. Therefore, it becomes important to critically question, if the status quo is the most suitable and efficient power distribution system for the future.

The main concept of microgrids is to include generation, storage, and load capabilities into a local distribution system, which can either operate in island mode or have a bidirectional power flow to the utility grid via a PCC. The system's power security, reliability, and quality can be improved since the microgrid can be disconnected from the grid in case of a fault situation. Kumar, Zare, and Ghosh [10] and Planas et al. [12] give a good overview of the possibilities of microgrids for different applications. The scientific publications of Noritake et al. [13] and Sannino, Postiglione, and Bollen [14] focus on the implementation of microgrids within office or commercial buildings.

To maximize the cost but also environmental efficiency of the microgrid, the grid structure should be optimized to match the connecting generating systems and loads. Those are linked with the distribution system through power converters, which make use of semiconductor devices to switch power and voltage levels to match the purpose of their respective application. When converting between ac and dc, an additional inversion or rectification stage is required. When operating the microgrid with dc, many of those ac-dc converters become negligible, due to the fact that many renewable energy sources like PV systems, storage systems like batteries, and electronic loads like all digital devices inherently require dc. Furthermore, modern motor loads and energy sources generating ac power are usually interfaced by a variable-speed drive to be decoupled from the rotor frequency, thus they can be connected via the existing dc-link to the microgrid. The elimination of converter components also eliminates their losses for the benefit of higher system efficiency. Various studies have demonstrated the significant potential of low-voltage dc microgrids regarding the reduction of energy transmission losses for a variety of different applications [3]. In particular, for office buildings with integrated renewable energy resources, Gerber et al. [15], Fregosi et al. [1] and Weiss et al. [16] prove the possibility of increased power efficiency. In order to evaluate those technology concept comprehensively, the environmental aspects of this paradigm chance should also be taken into account.

The LCA method is well established to holistically assess the environmental impacts and has been developed to evaluate the potential environmental impacts according to the entire life cycle of a product or a system. It is also standardized and regulated through the international ISO standards EN ISO 14040 [17] and EN ISO 14044 [18]. The framework of a full LCA consists of four iterative and interdependent phases: (1) goal and scope definition, (2) life cycle inventory (LCI), (3) life cycle impact assessment (LCIA) and (4) interpretation. If conducting comparative LCAs, the p

arts of the life cycle that accurately match in all compared systems may be omitted according to the black box method [19]. Databases with existing material flows are commonly used to model LCIs. However, power electronic components are only very rudimentarily represented in those databases and existing LCAs. The few modeled converters [20,21] are utilized regardless of application, topology and voltage class and additionally are discretely scaled to achieve the required power. As stated in the introduction part, with the current existing data basis, the level of detail required for the analysis of the environmental effects between ac and dc microgrids cannot be met.

Thus, for the closer examination and evaluation of systems based on power electronic components, current research is lacking the foundation of a technically sound database and methodology to adequately map the environmental aspects. Our study aims to address this research gap in order to answer our research question on what the environmental impacts of ac and dc microgrids are.

3. Methods and data

In this section, we present the method used for our analysis of the difference in environmental impacts of ac and dc microgrids. **Figure 2** depicts the observed systems for the ac (on the left) and dc (on the right) based microgrids including each electrical and motor loads, an appropriately sized PV and battery storage system, and the connection point to the public ac-based network (PCC). In accordance with the EN ISO 14040 norm [17], for the comparative LCA only the differences between the two systems are analyzed and are thus within the system boundaries of the LCA. On the one hand those are the differing components, so the difference in power converters and power distribution within the building, and on the other hand the difference in energy required from the connected public grid mainly due to differences in efficiency (represented as a red arrow connecting to the PCC in **Figure 2**). The design of the components including power requirements and energy demand as well as the amount of energy drawn from the public grid depend highly on the size and design of the building. Since this was an essential part of modelling the environmental impact of the ac and dc microgrids, a generic grid model was created to estimates those requirements and demands for the specifically chosen components.

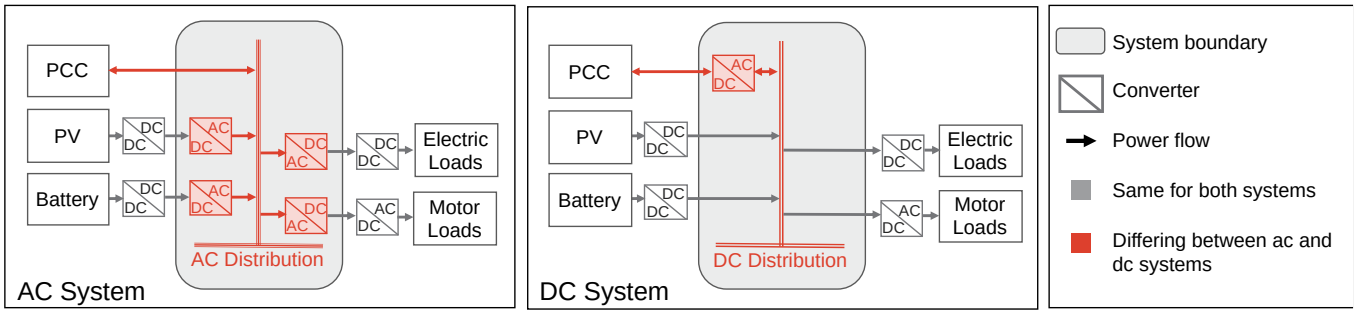

Figure 2: *System boundary graphs for the ac and dc system*

Therefore, in order to assess the environmental impacts for a broad range of building types, we combine a generic grid model for office buildings (subsection 3.1) with a model for the comparative LCA (subsection 3.2). Input variables and parameters are used to specify the type and size of the office building under consideration. This enables the generic grid model to create an energy and power balance for the chosen building and to determine the requirements for the building's power electronic components. In particular, the requirements for the number of components and their power and voltage levels are transferred to the comparative LCA model, where they are used to scale the environmental impact of the individual components. Thus, with the environmental impact of the individual components as well as the energy drawn from the public grid as outputs, the environmental impact of the entire system can be calculated. A graphical overview of this approach is shown in Figure 3. The generic grid model is described in more detail in subsection 3.1 and the comparative LCA in subsection 3.2.

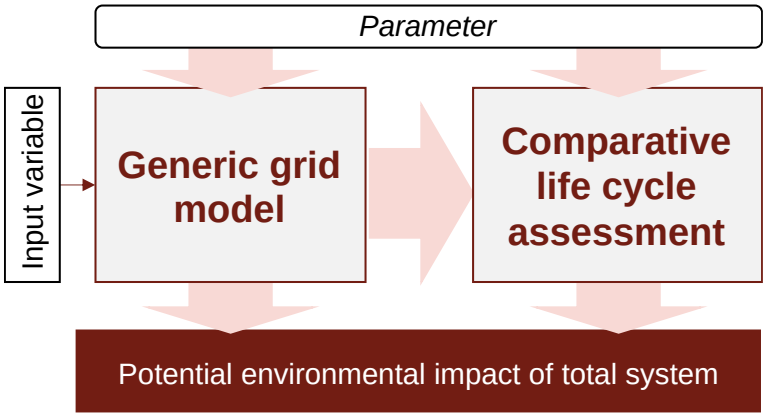

Figure 3: *Method of combining a generic grid model and an LCA*

3.1 Generic grid model

The application of a generic model aims to provide statements with universal validity about the power requirements and demands of an office building and thus the comparison of environmental impacts of dc and ac grids. Even though many office buildings have a similar structure, every building is unique considering size and layout. To ensure the broadest possible coverage among all alternatives, input variables and parameters are implemented. Figure 4 depicts a schematic overview of the generic grid model. The number of workstations (n_{ws}) is the primary input variable since it represents the main function of an office building. Additionally, the general layout of the building (shape), the number of floors and the different office (A_{Of}) and hallway (A_{hw}) area sizes[1] can be selected. Thus, different office building types, sizes and structures can be defined and evaluated.

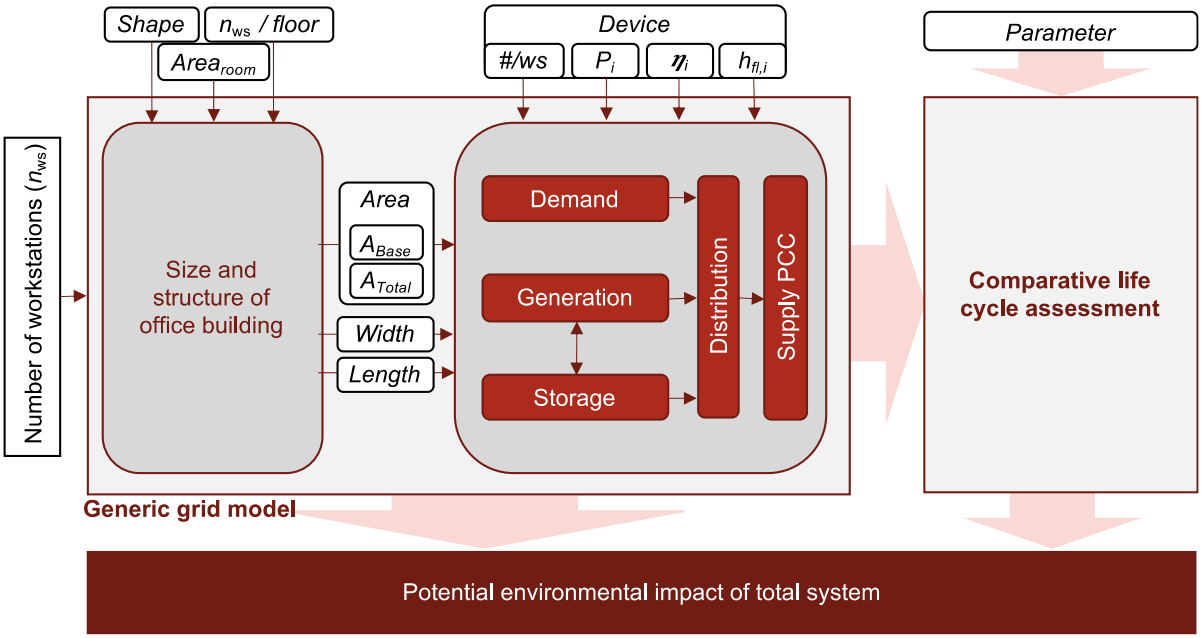

Figure 4: *Overview of generic grid model with variables and parameters*

[1] Range of area size in Table A.1 in Appendix A based on [22] given in [m^2]

In order to compare the grid structure and the required components, the electrical energy and power balance of the building is essential. This is based on a bottom-up approach considering the demand, generation, distribution and PCC. For the energy balance, the energy demand (E_{dem}) and generation (E_{gen}) including a estimation of storage potential, as well as the resulting required balancing energy from the public grid (E_{PCC}) are investigated. Furthermore, for the analysis of the power electronic components, an estimation of the power requirements for each considered component is needed.

The demand side consists mainly of the workstations with a computer and monitor, the lighting in the offices and corridors, and the centralized air conditioning and vent systems. The generation side is a PV-system which size varies with the available roof area and thus the base area of the building (A_{base}). The size of the battery storage is also dynamically estimated within the model in such a way that generated energy not directly consumed, e.g., at the weekend, can be utilized later to cover own demand. Different efficiencies for ac or dc-based distribution are taken into account. Combining demand and generation side under consideration of the differences in efficiency results in the amount of required energy from the public grid as well as the power requirements for the converter at the PCC in the dc based microgrid.

In the framework of the generic grid model, the key performance indicators and utilization of the observed devices can be adapted to the selected use case via parameters. Those are clustered into parameter classes with each being able to be scaled over a certain range. These parameter classes are the full load hours[2] (h_{fl}) for each device (index *i*) and each room type (index *j*), the nominal power (P) for each device, the efficiency of the connected power converter (η_i)[3] as well as the difference in efficiency between an ac and dc microgrid system (η_{acdc}). Taking into account the efficiency of the specific electric wiring system (η_{dist}), the annual energy demand (E_{dem}) can be calculated according to the number of workstations (n_{ws}) as stated in equation (1). The range of the parameters are listed in Appendix A.

$$E_{dem} = \frac{\sum_j (\sum_i \frac{P_i * h_{\mathrm{fl},i,j}}{\eta_i}) * n_{ws}}{\eta_{\mathrm{dist}}} \quad (1)$$

As described, the power electronic components are of particular interest for further consideration. Their individual power requirements and energy demand result from the generic model. Due to the individual requirements of these converters, different common topologies were used in each case.

The considered devices on the load side can be divided into electric and motor loads. The electric loads for this case are a personal computer (PC) and a monitor per workstation and additionally the overhead lighting in form of light-emitting diodes (LED)[4]. Their power per square meter depends on the standards that must be met for different room types according to DIN 12464-1 Table 5 [27]. The parts of the converter that can be removed when operating on a dc system are for all electrical loads a filter stage, a bridge rectifier consisting of four diodes, and a dc link capacitor. Additionally, the ad-dc converters for the PC and the LED require a power factor correlation (PFC) stage which is assumed to be embedded in a boost topology. The block diagram in Figure 5 depicts the typical structure of such a converter and in green the components that can be omitted for a dc microgrid. By operating on a dc microgrid, the efficiency of the converters can be improved by 4.5% for the PC, by 2.7% for the Monitor, and by 5.0% for the LED. [25,26]

[2] Range of full load hours in Table A.1 of Appendix A based on [22] given in hours [h]
[3] Range of efficiencies in Table A.2 of Appendix A given in percent [%]
[4] Range of Power given in watt given in [W] with the nominal power of the installed electric loads are 300 W for the PC, 70 W for the monitor and 39 W for the overhead lighting (cf. [23–26])

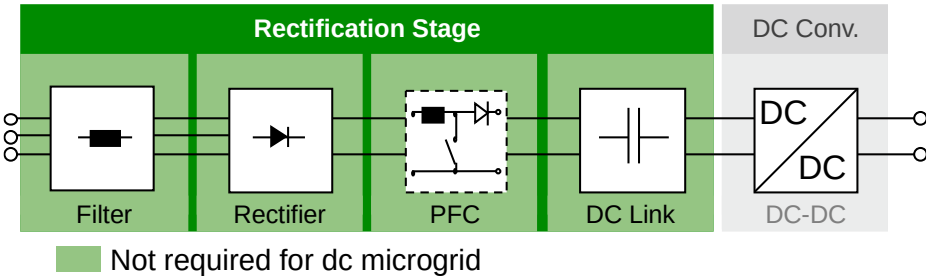

Figure 5: *Block diagram for a typical electric load converter connecting to an ac microgrid based on Stippich et al. [25]*

The motor loads consist of the centralized air conditioning and ventilation systems. The required power is estimated per square meter based on the norm VDI 3807 [22]. To be independent of the grid frequency, the converter consists of a rectification ac-dc stage, a boost dc-dc stage and an inversion dc-ac stage an ac microgrid as shown in Figure 6. For a dc microgrid the rectifying converter can be removed. Its topology is a voltage source inverter (VSI) consisting of six insulated gate bipolar transistors (IGBTs) parallel to freewheeling diodes and an efficiency of 95.0% [28]. With an input voltage of 230.0 V the output voltage at the dc link is $U_{\text{dc link}}$ = 538.2 V. Additionally, the dc link capacitor can be reduced.

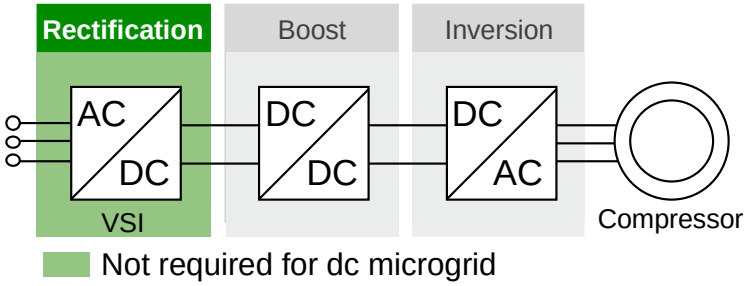

Figure 6: *Block diagram for a typical motor load converter connecting to an ac microgrid based on Webb [29]*

The generation side includes a PV-system combined with a battery storage, which is also connected to the interface of the ac microgrid by a dc-dc and a dc-ac converter. Comparable to the motor load converter, the dc-ac converter topology is assumed to be a VSI converter topology and can be omitted within a dc microgrid system. With the aforementioned efficiency, the dc system increases its efficiency for the motor load and the PV system by 5.0% and for the storage system by 9.8%, since the converter is utilized once when the energy is stored and once when it is fed back into the grid.

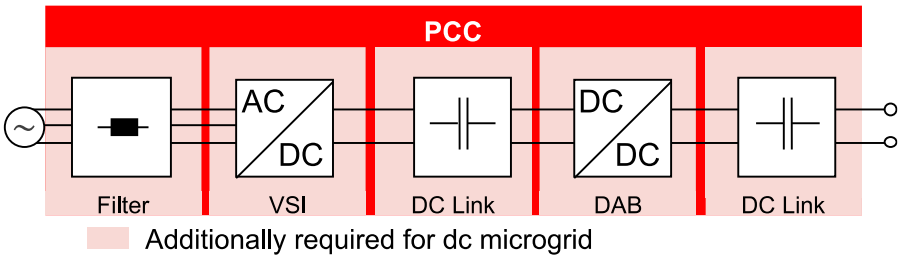

Figure 7: *Block diagram for a PCC converter required by a dc microgrid based on Kim et al. [30]*

The PCC balances the over- or underproduction of electrical energy via a bidirectional power flow to the public grid. The additional components for a dc microgrid consist of a filter stage, an ac-dc converter, a dc-dc converter and dc link capacitors as depicted in red in

Figure 7. The topology of the ac-dc converter is assumed to be a VSI, the one of the dc-dc converter a dual active bridge (DAB) based a prototype designs by Kim, Ryu, Baek, and Jung [30] and Naveen and Sekhar [31] and a topology design by De Doncker *et al.* [32]. The efficiency of the DAB is according to van Hoek and Shaker [33] around 93.0-98.0%, which leads to a total efficiency range of the PCC from 93.1% to 87.4%.

The design of the PCC converter is based on the maximum power (P_{PCC}) required, which can be defined by two cases: (1) there is no load and the generated PV electricity is fed completely into the public grid and (2) there is maximum load but neither PV nor battery can feed into the microgrid. In the first case, the converter must be designed in such a way that the power is greater than or equal to the maximum output of the PV system ($P_{PV,max}$). As equation (2) states this depends on the surface area of the building (A_{base}), the power of each PV module per square meter (P_{PV_module}), the efficiencies of the PV converter (η_{PV}) and the distribution system ($\eta_{distr,PV}$) as well as a PV utilization factor (f_{PV_util})[5].

$$P_{\mathrm{PCC}} \geq P_{\mathrm{PV\_max}} = \frac{P_{\mathrm{PV\_modul}} * A_{\mathrm{base}} * f_{\mathrm{PV\_util}}}{\eta_{PV} * \eta_{\mathrm{distr,PV}}} \quad (2)$$

In the second case, the maximum power of the load is calculated depending on the installed power of the components ($P_{n,inst,\,i}$)., their efficiencies (η_i, $\eta_{distr,i}$) and a simultaneity factor (g_i) as stated in equation (3). The simultaneous use of the devices is common in an office building and therefore the simultaneity factor for the electrical loads is assumed to be 95% [35].

$$P_{\mathrm{PCC}} \geq P_{\mathrm{dem\_max}} = \sum_{i \in devices} \frac{P_{\mathrm{n,inst},i} * g_i}{\eta_i * \eta_{\mathrm{distr},i}} \quad (3)$$

The power transmission is either realized through cable connections or a busbar system for higher currents [36]. The considered voltage level for the ac microgrid is the status quo three-phase 230 V. For the dc microgrid a 380 V unipolar bus distribution is chosen, as it reflects the most likely implementation [2,10]. The differences in employed material and efficiency of the electric wiring system is embedded in our model. Table 1 states the relevant outputs regarding area size, demanded and generated energy as well as the power levels calculated with the generic grid model exemplarily for a small office building with 50 workstations, a medium one with 150 workstations and 250 workstations representing a large building.

Table 1: *Calculated area, power and energy for a basic scenario of office buildings with 50, 150, and 250 workstations*

	Unit	Type of microgrid system	Small	Medium	Large
n_{WS}	Amount		50	150	250
A_{total}	m²		2 000	6 000	10 000
E_{PCC}	MWh/a	ac	-34[a)]	165	365
		dc	-76[a)]	142	356
		Difference	**42**	**23**	**9**

[5] According to Lödl et al. [34], this utilization factor 50% of the usable area can be utilized to installed PV module without shadowing other modules.

E_{gen}	MWh/a	ac	160	160	160
		dc	169	169	169
		Difference	**-9**	**-9**	**-9**
E_{dem}	MWh/a	ac	100	300	498
		dc	95	286	476
		Difference	**5**	**14**	**22**
P_{PCC}	kW	ac	160	261	426
		dc	168	248	414
		Difference	**-8**	**13**	**12**
P_{PV_max}	kW	ac	160	160	160
		dc	168	168	168
		Difference	**-8**	**-8**	**-8**
P_{dem_max}	kW	ac	87	261	436
		dc	83	248	414
		Difference	**4**	**13**	**12**

[a)] Feedings into the public grid are accounted for zero emissions within the LCA

3.2 Comparative life cycle assessment

The LCA is designed to be scalable with the grid model described in subsection 2.1 which is generically adaptable to different scenarios and use cases for office buildings.

Table 2 summarizes the parts, the relevant components consist of, which are within the system boundaries and, thus, are analyzed in the comparative approach. The differing components for the ac system are removed while the ones for the dc system are added. The final energy demand of the components (after the convertion step) is held constant to allow a fair comparison of both systems. Only the power flow in the distribution system and the PCC differs due to different efficiencies of components within the system. The applied comparative and scalable LCA approach in our study complies with international standardizations of the LCA method [17,18].

The goal and scope of the LCA are integrated into the overarching method of this study. The functional unit is the energy supply for the office building during the observed lifetime. The differing components and the electrical energy mix are looked at as subsystems. Their main output flows are the potential environmental impacts for the use of one of those converters or one kilowatt hour of electrical energy from the grid. The observed system is placed in Germany, and the time setting is 2018. The system lifetime can be chosen as one of the variables. Since most inverters and transformers are considered to have a lifetime of 23 to 30 years, this range is a good basis for the lifetime for the observed system [20]. The lifespan of each component is part of the parameter class lifetime of the generic grid model. We utilize the database *ecoinvent 3.4* (2017) as basis for the inventory analysis and integrate and adjust it within the open source software *openLCA* for the calculations [37].

Table 2: *Dependencies between mass or area and power and/or voltage level of component*

a) Derived from fundamental electrotechnical equations shown below

Component	Dependency	Source
Printed Circuit Board (PCB)	$A_{\mathrm{PCB}} \sim \sqrt[0.68]{\frac{P_{\mathrm{PCB}}}{U_{\mathrm{PCB}}}}$	a)
Resistor	$M_{\mathrm{res}} \sim \frac{P_{\mathrm{res}}}{{U_{\mathrm{res}}}^2}$	a)

Transformer	$\frac{M_{\text{ferrite trans}} \sim P_{\text{trans}}^{\frac{6}{7}}}{M_{\text{copper trans}} \sim \sqrt[3.5]{P_{\text{trans}}}}$	a)
Cables/Busbar	$M_{\text{copper cable}} \sim \frac{P_{\text{distribution}}}{U_{\text{distribution}}}$	a)
Capacitor	$M_{\text{capacitor}} \sim \frac{P_{\text{capacitor}}}{U_{\text{capacitor}}}$	Based on Nordelöf *et al.* [9]
Heat sink	$M_{\text{heat sink}} \sim P_{\text{heat sink}}$	Based on Nordelöf *et al.* [9]
Power Module	$M_{\text{power module}} \sim P_{\text{converter}}$	Based on Nordelöf *et al.* [9]

Existing LCIAs for power electronics are generally integrated into LCAs by discretely scaling the whole converter with the required power level, e.g., in [20] and [21]. This does not meet the level of detail required by the technology comparison conducted in our study as stated in the introduction part (1). Thus, our comparative LCA is designed in such a way that the employed material compositions of the components within a converter are proportional to the power and/or voltage levels. For this, fundamental equations have been derived which are based on the underlying physics. With that, our study creates a basis for the derivation of LCAs for power electronics, in which the components can be selected according to a modular principle and scaled continuously to meet the applicable requirements.

The components of each power electronic converter are observed individually and can then be assembled according to their specific topology, as well as power and voltage level. Thus, the LCA is scalable and adjustable to the chosen use case and can be integrated into the analysis of the energy system at a higher level. Power electronic converters cover a broad range of applications and therefore differ enormously in terms of size and material composition. Since the main components scale in size with power and voltage levels, a modular design approach enables an appropriate approximation of their actual environmental impact. The dependencies of the mass (*M*) or area size (*A*) of the main power electronic components and the distribution system to their power (*P*) and voltage (*V*) levels are summarized in Table 2.

If for **the printed circuit board (PCB)** the required sizes cannot be either taken from literature, assumptions on the basis of the size of the mounted components or manuals, a scaling assumption according to the current-carrying capacity of the board is made. The norm IPC-2152 states that the required area of the current tracks ($A_{\text{PCB ct}}$) depends on the current capacity ($I_{\text{PCB ct}}$) according [38]. The assumption is made that the area of the entire PCB (A_{PCB}) has that same dependency on the current flowing through the PCB (I_{PCB}). The dependency in Table 2 represents accordingly the ratio between current to the base current ($I_{\text{PCB base}}$) and the size of the base module ($A_{\text{PCB base}}$) under the assumption that equal temperatures apply.

To scale the mass of a **resistor**, the fundamental formulas for resistors are observed in Equations (4) and Fehler! Verweisquelle konnte nicht gefunden werden.. They state that the resistance (*R*) is equal to its squared voltage (U_{res}) divided by its power (P_{res}), and also equal to the resistor length (l_{res}) divided by the resistors cross-section area ($A_{\text{cs res}}$) times the electrical conductivity (σ_{res}). Those equations are combined with the formula for the volume of a component in Equation Fehler! Verweisquelle konnte nicht gefunden werden. and the mass in Equation Fehler! Verweisquelle konnte nicht gefunden werden. depending on the electrical conductivity and material density (ρ_{material}). The resulting relationship between the mass of a

resistor (M_{res}) and the power and voltage that applies to it, is stated in Equation (8) with the scaling factor being α_{res}.

$$R = \frac{(U_{\text{res}})^2}{P_{\text{res}}} \tag{4}$$

$$R = \frac{l_{res}}{A_{\text{cs res}}} * \sigma_{\text{res}} \tag{5}$$

$$V_{\text{res}} = A_{\text{cs res}} * l_{res} = \frac{(l_{\text{res}})^2}{R} * \sigma_{\text{res}} \tag{6}$$

$$M_{\text{res}} = V_{\text{res}} * \rho_{\text{material}} = \frac{{l_{\text{res}}}^2}{(U_{\text{res}})^2} * P_{res} * \sigma_{\text{res}} * \rho_{\text{material}} \tag{7}$$

$$M_{\text{res}} = \alpha_{\text{res}} \frac{P_{\text{res}}}{(U_{\text{res}})^2} \tag{8}$$

The active materials used in a **transformer** are ferrite for the core and copper for the windings. If the design of a **core** is known for a certain power level, the weight of it can be calculated or looked up in datasheets. According to the law of similarity the scaling of the dimensions of the transformer by the factor β, while keeping a constant design and frequency, leads to an adjusted volume (V_{core}) by the factor β^3 and adapted area and therefore mass ($M_{ferrite}$) by factor β^3 (see Equation (9)). Under the considerations of the laws for the magnetic fields of the transformer, the scaling of the transformer by β leads to a power increase by $\beta^{3.5}$ between the power of the base transformer (P_{base}) and the adjusted transformer (P_{trans}) as depicted in Equation Fehler! Verweisquelle konnte nicht gefunden werden. [39]. Thus, the mass of the core is estimated by the Equation Fehler! Verweisquelle konnte nicht gefunden werden. when scaling over the power of the transformer.

$$V_{\text{core}} \sim M_{\text{ferrite}} \sim \beta^3 \tag{9}$$

$$\frac{P_{\text{trans}}}{P_{\text{base}}} \sim \beta^{3.5} \tag{10}$$

$$M_{\text{ferrite}} = \sqrt[3.5]{\left(\frac{P_{\text{trans}}}{P_{\text{base}}}\right)^3 * {M_{\text{ferrite base}}}^{3.5}} \tag{11}$$

The mass of copper for transformer **windings** is defined as the material density (ρ_{cu}) times the volume of the wire (V_{wire}), which can be calculated by the sum of the area of the wire cross-section ($A_{cs\ wire\ k}$) times the number of turns ($N_{Min\ k}$) and length of one turn ($l_{N\ k}$) for each primary and secondary side as stated in Equation (1). The number of turns can be calculated according to Equation (2) based on the applied voltage (U_k), the switching frequency (f), the cross-section area of the wire, and the change in magnetic flux density (ΔB). The cross-section area can be calculated by dividing the current by the maximum current density of copper ($J_{cu\ max}$). The maximum change in magnetic flux density is for 50 kHz switching frequencies around 0.25 Tesla [40]. When scaling to a different power level, the voltage, frequency, and change in magnetic flux density are assumed to stay constant, and thus, the number of turns only depends on the cross-section area of the wires. That area depends on the current (I_k). With a constant current density of copper, the cross-section area of the wire is proportionality with the power as shown in Equation (3). With the proportionality of the number of windings and the cross-section areas that cancel each other out, the mass concludes to be proportional only to the length of one winding, which itself is proportional to the scaling

factor β as shown in Equation (4). Thus, the copper mass of a transformer ($M_{\text{cu trans}}$) can be calculated with Equation (5). With those formulas, the copper amount can be determined for a base data point and then scaled accordingly to the required power voltage.

$$M_{\text{cu trans}} = \rho_{\text{cu}} * V_{\text{wire}} = \rho_{\text{cu}} * \sum_{k} A_{\text{cs wire } k} * N_{\text{min } k} * l_{\text{N } k} \tag{1}$$

$$N_{k\,\text{min}} \geq \frac{U_k * \frac{1}{2\,\text{f}}}{\Delta B * A_{\text{cs wire k min}}} \sim \frac{1}{A_{\text{cs wire k min}}} \tag{2}$$

$$A_{\text{cs wire } k} = \frac{I_k}{J_{\text{cu}}} \sim P \tag{3}$$

$$M_{\text{cu trans}} = A_{\text{cs wire}} * N_{\text{min}} * l_{\text{N}} * \rho_{\text{cu}} \sim l_{\text{N}} \sim \beta \tag{4}$$

$$M_{\text{cu trans}} = M_{\text{cu base}} \sqrt[3.5]{\frac{P_{\text{trans}}}{P_{\text{base}}}} \tag{5}$$

The current carrying capacity limits for **cables** depend greatly on external properties such as installation type or operating temperature. That is why the required cross section for cables are calculated by the allowed voltage drop (ΔU_v), which is 3% for low voltage systems according to VDE 0100-520 [41]. The voltage drop can be determined based on the distributed power (P_{distr}) and voltage (U_{distr}), the cable is supposed to transmit, and the cable resistance (R_{cable}), which depends on the cable length (l_{cable}), the specific conductivity of copper (σ_{cu}), and the cross section of the wire ($A_{\text{cs wire}}$). According to the different current and voltage dependencies of single-phase ac, three-phase ac, and dc power supply, the voltage loss can be calculated according to formula (17) or (18) respectively, and converted to calculate the required cross section by Equations (19) or (20) The required cross-sections are then rounded up to the standard cross-section according to VDE 0295:2005-09 [42]. The efficiency of the distribution system concludes on the resulting voltage drop with the adjusted wire cross-section. The plugs are considered to have an equally irrelevant difference. The other distribution systems showed much more relevant differences and will be taken into account. It has to be stated, that this estimation should be simultaneously considered with the current carrying capacity for cables and the relevant standards, and it cannot replace a detailed calculation. [43]

$$\Delta U_{\text{v dc}} = \Delta U_{\text{v ac\_1p}} = 2 * \frac{P_{\text{distr}}}{U_{\text{distr}}} * R_{\text{cable}} = 2 * \frac{P_{\text{distr}}}{U_{\text{distr}}} * \frac{l_{\text{cable}}}{A_{\text{cs wire}} * \sigma_{\text{Cu}}} \tag{17}$$

$$\Delta U_{\text{v ac\_3p}} = \frac{P_{\text{distr}}}{U_{\text{distr}}} * \frac{l_{\text{cable}}}{A_{\text{cs wire}} * \sigma_{\text{Cu}}} \tag{18}$$

$$A_{\text{cs wire dc}} = A_{\text{cs wire ac\_1}P} = \frac{2 * l_{\text{cable}} * P_{\text{distr}}}{\sigma_{\text{Cu}} * \Delta U_{\text{v}} * U_{\text{distr}}} \tag{19}$$

$$A_{\text{wire ac\_3p}} = \frac{l_{\text{cable}} * P_{\text{distr}}}{\sigma_{\text{cu}} * \Delta U_{\text{v}} * U_{\text{distr}}} \tag{20}$$

A **busbar trunking system** is assumed for the main vertical and horizontal distribution within the office building, if the current is above 1,600 A. Those systems have the advantages of good extendibility, a high operational safety and are easily assembled [36]. As Equations *(*6) show, the required copper cross-section area of the *busbars* ($A_{\text{cs busbar}}$) can be calculated over the flowing current (I_{dist}) and the current carrying

capacity of copper ($J_{cu\ max}$). According to manufacturers, copper can withstand currents approximately around 5 A/mm^2 per single conductor with an additional 5% as safety factor compensating for the compound heat gain within the conductor for every additional conductor in the bus assembly (see Equation (22), with N being the total numbers of conductors in the bus assembly) [44]. The mass of the busbar can be calculated via the cross-section area, and thus is depended on the current (I_{dist}) or the distributed power (P_{dist}) divided by the voltage (U_{dist}) as stated in Table 2. The power losses (ΔP) of the system are equal to the square of the current (I_{dist}) times the residence of the conductor (R_{busbar}) as shown in Equation (23), with a specific conductivity of copper (σ_{cu}) at a temperature of 20° C is 56.0 m/(Ω*mm^2)[6]. In general, the design and size of busbars are only estimations, and a more precise thermal simulation should be conducted when designing a busbar trunking system.

$$A_{\mathrm{cs\ busbar}} = \frac{I_{dis}}{J_{\mathrm{cu\ max}}} \tag{6}$$

$$J_{\mathrm{cu\ max}} = \frac{5\ \mathrm{A/mm^2}}{1 + 0.05 * (N-1)} \tag{22}$$

$$\Delta P_i = (I_{\mathrm{dis}\,i})^2 * R_{\mathrm{busbar}\,i} = (I_{\mathrm{dis}\,i})^2 * \frac{S_i}{\sigma_{\mathrm{cu}} * A_{\mathrm{cs\ busbar}\,i}} * l_{\mathrm{busbar}\,i} \tag{23}$$

Semiconductor devices like diodes and transistors are responsible for the actual switching of the converter. They have to be operated within the voltage and current limits, which they are designed for. To achieve higher limits, they can either be connected in parallel (higher current carrying capacity) or in series (higher voltage stability) or different technologies with higher robustness have to be applied. Therefore, those components cannot be scaled continuously but only discretely. For higher-power converters, the semiconductors are integrated into a power module. Nordelöf *et al.* states a detailed scalable LCIA for such a power module with a VSI topology [9].

The dependencies between the masses of the **capacitor** and the **heatsink** according to their power and voltage levels are indicated. Furthermore, the aforementioned study lists the materials for the **driver** and **logic boards** which are assumed to scale discretely. Those findings are included in the modeling of this study as shown in Table 2. The compositions of the individual components of the power converters are described in Appendix B. Additionally, the **transportation** of the components is based on the global default data for electronic components and boards by the ecoinvent database [45].

To consider the environmental impacts of the varying purchase of **electricity** from the public grid caused by differing efficiencies of dc and ac microgrids, the electric energy mix is modeled. In addition to Germany's electricity mix in 2017 according to Fraunhofer ISE [46], possible electricity mixes for the years 2030 and 2050 are considered, which are based on scenarios with accelerated electrification, increased energy efficiencies and result in fulfillment of the climate mitigation targets [47]. The scenarios result in an optimistic utilization rate of renewable energies of 66% for 2030 and more than 90% for 2050, and thus, the three compilations under consideration offer a wide variation. To model the electricity mixes the datasets “market for electricity, low voltage” and “market for electricity, high voltage” for the German market within the *ecoinvent* database have been adjusted [48,49]. Figure 8 depicts the resulting percentages of the different generation units and the difference to the original datasets of the *ecoinvent* database.

[6] The factor S takes the skin and proximity effects into account, which have to be considered for higher currents in an ac system. These effects is complex and is dependent on a variety of variables itself. The simplified approach based on Chapman and Norris (2018) is stated in Appendix C.

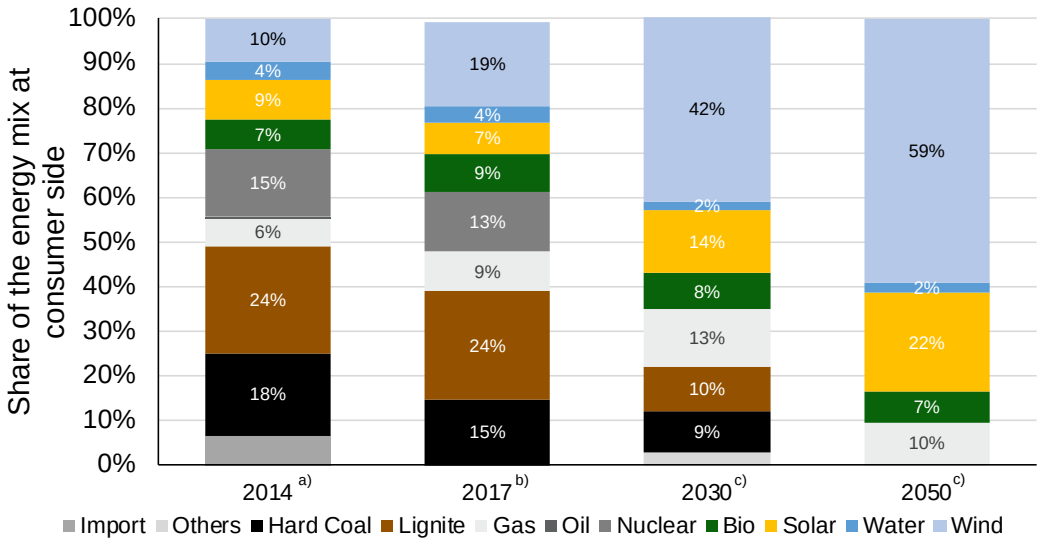

Figure 8: *Share of energy mix at consumer side in Germany for different years based on a) Wernet et al. [37]), b) Fraunhofer ISE (2018) [46] and c) Hecking et al. [47].*

To evaluate the materials and processes used in the LCIA, the impact assessment method *ReCiPe 2016 Midpoint H* is chosen [50]. Mainly the impact category climate change measured in tons of carbon dioxide equivalent (t CO_2 eq) is evaluated. Other impact categories are monitored as well to detect a potential shift in environmental impacts.

4. Results

To evaluate the results, three different building sizes are observed – a small one with 50, a medium one with 150, and a large one with 250 workstations.

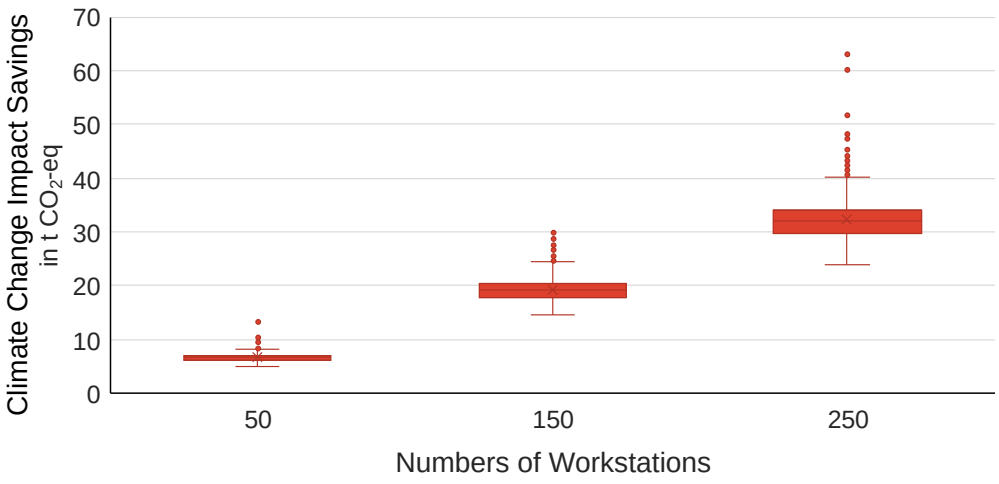

Figure 9: *Range for the differences of impacts of climate change on three different building sizes generated with a Monte Carlo simulation (1000 runs)*

First, the climate change impacts of the differing components between the ac and dc system are analyzed without including the impacts of the energy supply from the public grid. A *Monte Carlo* simulation is conducted to investigate all possible cases that may arise from the previously defined parameter ranges as mentioned in section 3.1. The following results show the savings that would be possible with a network

based on direct current, i.e., different from the status quo. Positive values are indicating that the dc-based system can save emissions, while negative values show that the ac based system might be superior. Figure 9 depicts the climate change emissions that can be avoided in small, medium, and large office buildings for the differences of components when utilizing a dc microgrid instead of an ac one.

Under consideration of all uncertainties, the emissions for the removed components are higher in all cases than the ones of the additionally added components for the PCC. Therefore, the installation of a dc microgrid system can reduce greenhouse gas emissions of the involved components, due to an overall material reduction. Meaning emissions saved due to the removed components is higher than those added due to the additional required converter at the PCC. At the same time, this shows the range for safety measures components within a dc grid – which are currently subject of research – so that the dc-based grid continues to have lower greenhouse gas emissions in production than the ac grid. Even with some outliers, it can be concluded that the potential reductions in CO_2 eq emissions scale with the size of the buildings, due to a rising number of reduced components (i.e., a bigger levy). The main driver for CO_2-eq. emissions for the components are the aluminum for the heatsinks, the copper for the inductor and transformer and the iron for the transformer. So especially the materials with an energy-intensive production.

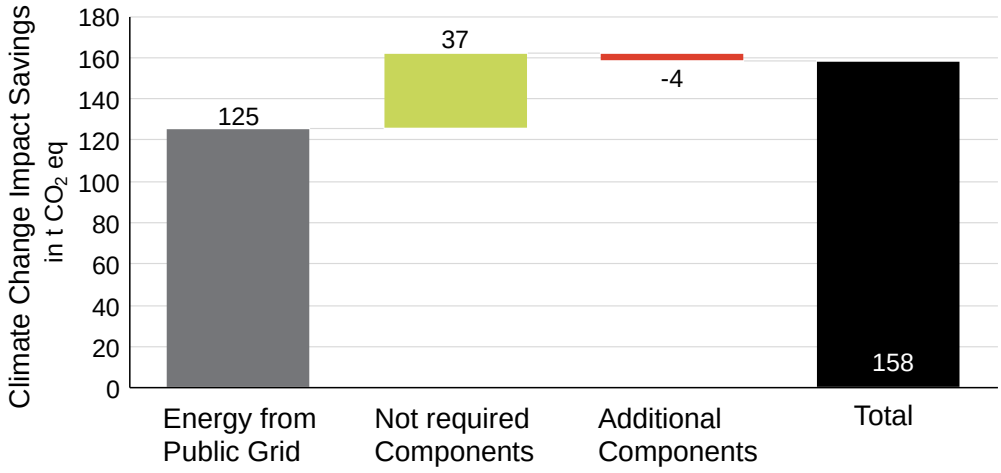

Figure 10: *Potential climate change impact savings for a dc microgrid system with 250 workstations*

For a comprehensive view, the differences in electrical energy supplied by the public grid for the two systems must also be taken into account. Figure 10 shows exemplarily the climate change impact savings of a dc microgrid for an average scenario of a building with 250 workstations. It becomes apparent that the emissions of the energy supplied by the public grid have a more substantial influence on the potential emission savings than the removed or added components, i.e., the use phase has a higher climate change impact in case energy from the public grid is required than the production phase.

However, for the other impact categories of the applied ReCiPe 2016 (H) method this cannot be generalized as the results for the same average scenario for a building with 250 workstations depicted in Figure 11 show. In particular, it can be observed that mineral resource scarcity, fine particulate matter, terrestrial acidification, human non-carcinogenic toxicity, and terrestrial ecotoxicity have a greater impact during the production phase than the use phase. The different impact categories were analyzed for the other scenarios as well as across the parameter ranges. In all these cases the results were greater than zero, which means that the dc-based system has less environmental impact than the ac system for all cases. With an increased share of renewable energies in the electricity mix, the environmental impact in

the categories mineral resource scarcity and terrestrial ecotoxicity rise. However, since the dc-based systems are in most cases more energy efficient, no negative values are observed here either.

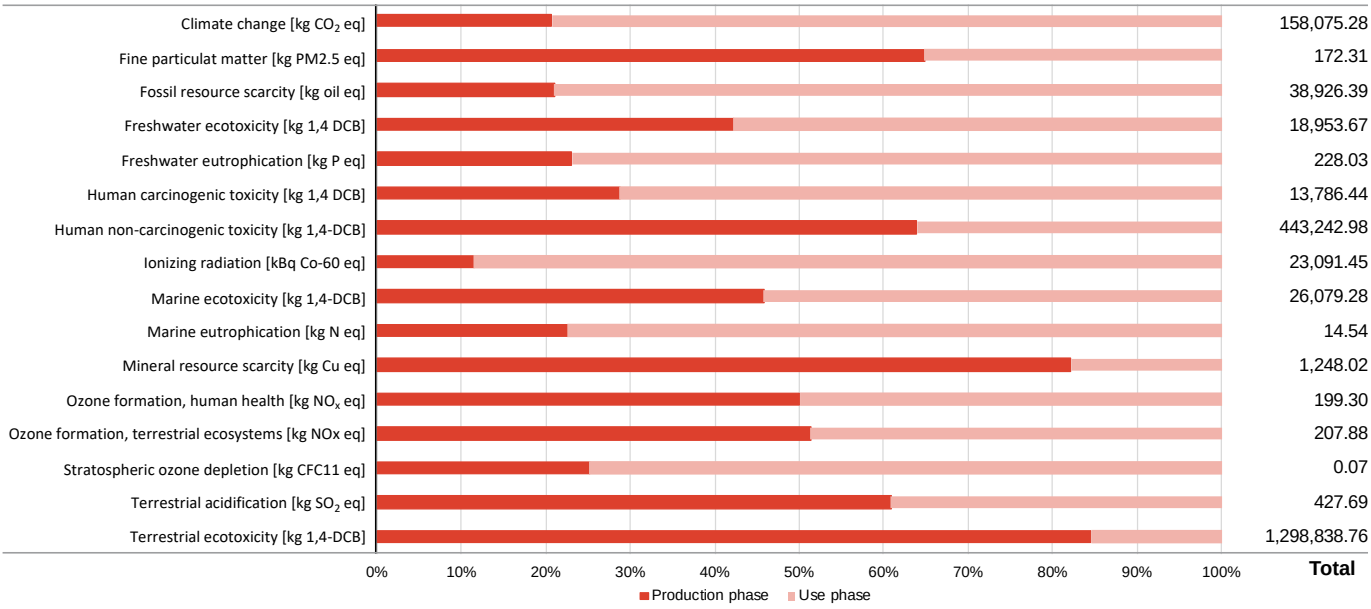

Figure 11: Results for other impact categories for the ReCiPe 2016 (H) method exemplarily for a building with 250 workstations divided by the impact during the production phase (due to the differing components) and the use phase (due to the difference in required energy from the public grid)

In order to further investigate these observation, sensitivity analyses for the parameters nominal power (P), efficiency (η), and full load hours (h_{fl})[7] were performed by varying the observed factors between the five levels of their range *ceteris paribus*. In the average scenario, the smaller building with 50 workstations can supply itself autarkically, and therefore only the emissions that can be saved due to the changed components can be reduced with a dc-based grid design. As depicted in Figure 12, electricity from the public grid is only required when the existing appliances are operating at higher power, thus the potential savings in emissions is increased. The other two example buildings draw electricity from the public grid in every use case, and the potential climate change emission savings decrease with utilization of higher power components as much that there is a case where the ac microgrid has fewer climate change emissions than the dc one. This is due to the efficiency losses of the PCC converter, which becomes more significant in absolute terms when more electricity is drawn from the public grid. This can be also observed for the variation of the parameter efficiency (h) as depicted in Figure 13. With higher efficiencies from the converter, the dc microgrid is environmentally more favorable than the ac grid. The effects when varying the parameter full load hour (h_{fl}) are similar except the variation only has an influence on the amount of energy used within the building not on the design of the components itself. Those analyses confirm that energy from the public grid is the main driver for climate change emissions. Furthermore, the results indicate that the environmental impact differences between dc and ac microgrids are highly dependent on the utilization, structure, and layout of the building, as this effect the potential usage of rooftop PV.

[7] The full parameters ranges are stated in Appendix A

Especially, high efficiencies of dc microgrid components and large generation capacities of renewable energies within the building result in reduced potential environmental impacts.

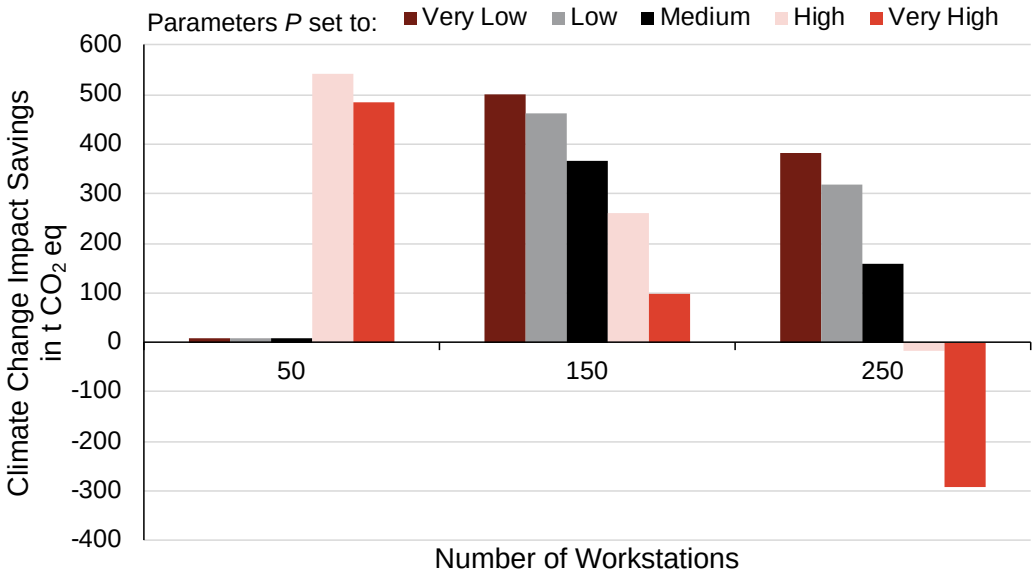

Figure 12: *Climate Change impact savings of sensitivity analysis for parameter power*

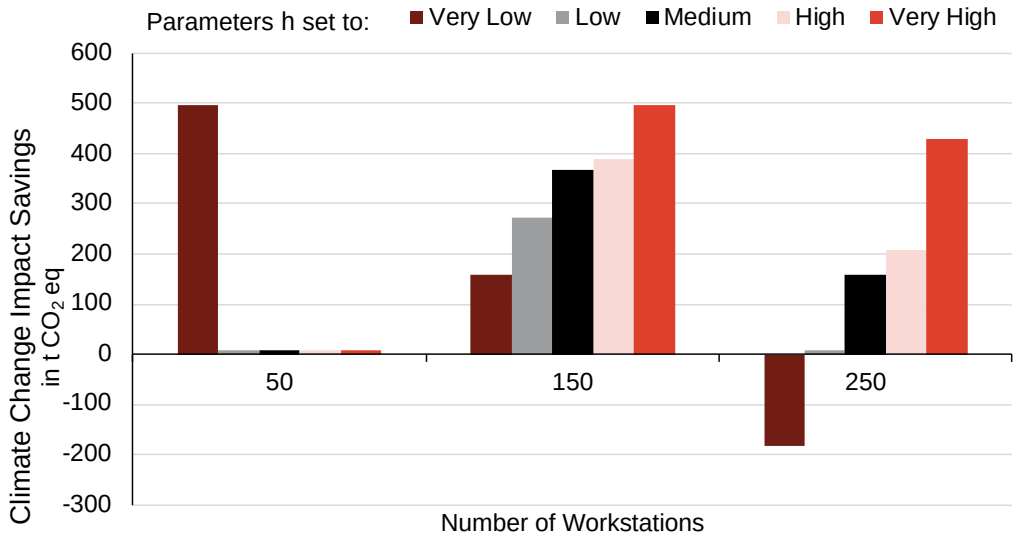

Figure 13: *Climate change impact savings of sensitivity analysis for parameter efficiency*

In order to cover uncertainties in the feasibility of implementing the dc components, ranges in material usage were taken into account. These uncertainties show only smaller influence on the overall emissions with a deviation from the standard use case of a maximum of 5.0%. As the main driver for climate change emissions, the electricity mix, is observed separately. Based on the possible future scenarios for electricity mixes in 2030 and 2050 the emissions can be cut by one third or two thirds respectively compared to the basic scenario in case the microgrid requires energy from the public grid as depicted in Figure 14. Therefore, the emissions saved when using a dc-based microgrid instead of an ac-based one decreases. An increase in renewable energy resources within the energy mix results in an increased impacts of mineral resource scarcity and terrestrial ecotoxicity. When observing those impact categories for the basic scenario the total results of the system stay above zero, as well as for all the other impact categories. Therefore,

the dc microgrid can reduce environmental impacts for all observed impact categories when compared to ac microgrids in the basic scenario.

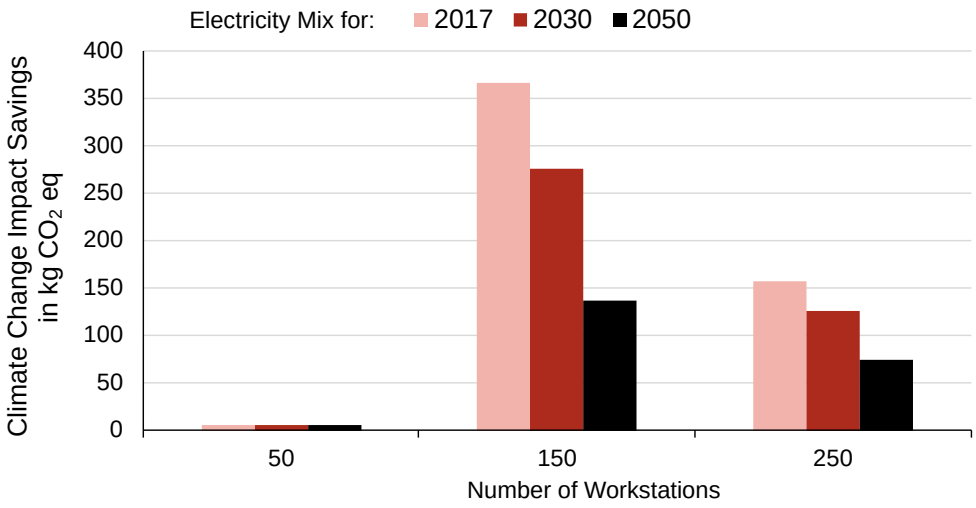

Figure 14: *Climate change impact savings of sensitivity analysis for different electricity mixes*

For the analysis, the scaling of the power electronic components – contrary to currently often applied method of discrete scaling – it was carried out her more realistically via the parameters power and voltage as explained in chapter 3.2. The differences in results when applying these different scaling methods, is here presented for a ac-dc stage. The continuous scaling over power is compared to a discrete scaling of inverter blocks with 20 kW and 50 kW showed exemplarily for the PCC converter in Figure 15. The results for climate change impact increases much faster with a discrete scaling especially for inverter blocks with smaller power levels. This is because neither the size of the housing, the heatsink, the IGBT module nor DAB increase in reality linearly with the power. This demonstrate evidently that there is a need for a detailed investigation – deviating from the status quo of discrete scaling – when comparing environmental impacts of different concepts for power electronic components.

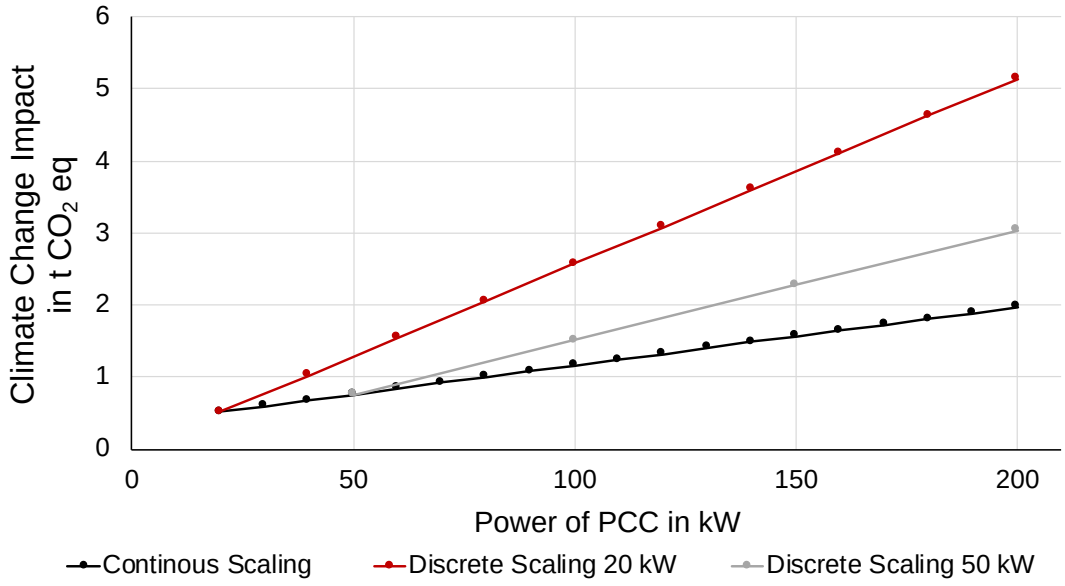

Figure 15: *Climate change impact of a PCC converter with different applied scaling methods*

5. Discussion

Our study analyzes the difference in environmental impact of microgrids either operated on dc or ac. In order to investigate this, we designed the model and its components according to the energy and power requirements of the building. A broad generic grid model with a large number of parameters was used to cover as many variations as possible. The environmental impact of the components within a microgrid was identified. As our research indicates, particularly the electricity mix has a substantial influence on the climate change impact. Therefore, further analyses with a time-resolved model could provide insights into additional emission reduction potentials. As the sensitivity analysis shows, the steady decarbonization of the energy mix leads to a reduction of the system's emissions in general. However, this decreases the potential of dc microgrids to reduce emissions compared to an ac one. The realization of a decarbonized energy system, in turn, requires modified system structures to ensure power security, reliability and quality, which dc microgrids can support as discussed in section 2. The analysis of other significant impact categories ensured that the technology change will not cause a shift of environmental impacts. Though, with an increased integration of renewable energies, the impacts on mineral resource scarcity and terrestrial ecotoxicity rise and should be considered in future works.

Furthermore, our analysis of the individual components shows that the production processes, and with that the energy they require, are mainly responsible for the emissions. Thus, those processes are inextricably linked to the energy mix of the country they are produced in. With increasing decarbonization of the energy systems, those emissions can be reduced as well. A more detailed analysis from which countries the materials are imported and thus, which energy mix is utilized could further specify the comparison of environmental impacts. This becomes particularly important for materials that require a significant amount of energy during the production e.g., aluminum.

Our analysis shows that the environmental impacts can be reduced on the component level for all relevant impact categories. Thus, dc microgrids increase resource efficiencies since they provide at least the same utility as ac microgrids. Due to the reduced use of material, the material costs can be lowered as well for all observed cases. However, a more accurate economic assessment including the production costs should be included.

As a first approach towards a scalable LCA of power electronic components integrated into an energy system, simplifications had to be made. Due to a technically unsound data basis, fundamental models first had to be derived in order to identify the environmental impact of the components. In particular for buildings with higher connecting power, a different convert topology could be useful for the PCC.

As a relatively new concept, there are still no standardizations regarding filter circuits and protection systems for low-voltage dc technology and therefore they are not yet integrated into the model. Without the voltage zero crossing of ac voltage, occurrences of stable burning arcs within a dc system cannot be trivially disconnected. Thus, more complex power switches or disconnectors are required ([2]). Kumar et al. [10] and Hirsch et al. [51] give a good overview of the current status of the technological and standardization developments for microgrids. Additionally, the VDE Standardization Roadmap for Low Voltage dc highlights the standardization process in Germany [52]. The environmental impacts of these components should be compared to the corresponding technologies in an ac system for a comprehensive assessment. Overall, the estimated climate change impact savings represent the maximum margin that these components can have in order to ensure that a dc microgrid stays at least climate change neutral compared to an ac microgrid.

There are only very few scientific publications in the field of LCAs for power electronics to compare our results to. In particular, the environmental impacts of power electronics integrated into systems have not yet been investigated. However, components for electrical devices have been examined. The database ecoinvent includes the dataset "*power supply unit production – for desktop computer*" which is the entire converter stage for a computer. For a better comparability, the dataset is adjusted to only include lead-free PCBs. Evaluating this adjusted dataset with the same impact assessment method, the climate change impact results to 42.2 kg CO_2 eq. The results for the removed parts modeled in this manuscript summed up to approximately 25% of that value with 10.9 kg CO_2 eq. Considering the fact that the PCB was reduced by one fourth, those values seem reasonable. The main drivers of the ecoinvent dataset are the mounted PCB causing 88% of the climate change emission. Investigating the mounted components on that board, shows that the inductor coils account for 22%, the transistors for 11%, the empty PCB board for 20% and the capacitor for 9%. Our component analysis showed that the inductor coil contributes to the climate change impact emissions with 56%, followed by the bridge rectifier with 11% and the PCB with 9%. While the percentages differ in the results of our research, the main drivers are the same and therefore, the results seem reasonable.

6. Conclusion and outlook

Our study identified and analyzed the environmental impacts of dc microgrids compared to ac microgrids within office buildings under consideration of their entire life cycle. A shift from ac to dc microgrids would especially entail a substantial reduction in material usage and thereby increase resource efficiency. In turn, such a substantial reduction in materials would result in reductions of greenhouse gas emissions as well as reductions in other relevant impact categories for all observed scenarios for the production phase. We identified the electricity drawn from the public grid as main driver for the difference in emissions in the life cycle analysis. Efficiency gains lead to an overall decrease in energy demand of a dc system compared to an ac system. Therefore, they have a substantial leverage effect on reducing emissions. Thus, particularly the PCC converter must operate with a high efficiency. The sensitivity analyses demonstrate that the differences in environmental impacts between dc and ac microgrids are highly dependent on the utilization, structure, and layout of the building and the efficiency of the converter.

Our method enables a detailed analysis of the environmental impacts of power electronic components. Thus, it lays the foundation for an evaluation criterion for a comprehensive assessment of technological changes. It can be used as a basis to evaluate further designs of microgrids such as the integration of further components, other topologies, safety, and different voltage levels. Furthermore, the detailed investigations of the environmental influences of power electronics can be transferred to other fields of application, e.g., production process, mobility, or infrastructure, particularly as an additional criterion for the selection of technologies.

In addition, our method could be integrated into a systemic approach in order to obtain insights focusing on the environmental impacts of a paradigm shift from ac to dc on an aggregated level. For further analyses, such an approach would have to take into account ongoing changes in the energy system, the resulting composition of the energy mix and the origin and production of components and their materials. Based on this, the systems could be compared in terms of their resource efficiency, especially with regard to finite resources and materials with high energy requirements during production.

Funding

This research did not receive any specific grant from funding agencies in the public, commercial, or not-for-profit sectors.

References

[1] Fregosi D, Ravula S, Brhlik D, Saussele J, Frank S, Bonnema E, et al. A comparative study of DC and AC microgrids in commercial buildings across different climates and operating profiles, IEEE; 2015, p. 159–64. https://doi.org/10.1109/ICDCM.2015.7152031.

[2] Ott L, Wunder B, Han Y, Kaiser J, März M. Power Electronics for Low-Voltage DC Grids in Commercial Build- ings, Research Gate; 2014.

[3] De Doncker RW. Power electronic technologies for flexible DC distribution grids, IEEE; 2014, p. 736–43. https://doi.org/10.1109/IPEC.2014.6869670.

[4] Wang R, Lam C-M, Hsu S-C, Chen J-H. Life cycle assessment and energy payback time of a standalone hybrid renewable energy commercial microgrid: A case study of Town Island in Hong Kong. Appl Energy 2019;250:760–75. https://doi.org/10.1016/j.apenergy.2019.04.183.

[5] Das J, Abraham AP, Ghosh PC, Banerjee R. Life cycle energy and carbon footprint analysis of photovoltaic battery microgrid system in India. Clean Technol Environ Policy 2018;20:65–80. https://doi.org/10.1007/s10098-017-1456-4.

[6] Smith C, Burrows J, Scheier E, Young A, Smith J, Young T, et al. Comparative Life Cycle Assessment of a Thai Island's diesel/PV/wind hybrid microgrid. Renew Energy 2015;80:85–100. https://doi.org/10.1016/j.renene.2015.01.003.

[7] Papageorgiou A, Ashok A, Hashemi Farzad T, Sundberg C. Climate change impact of integrating a solar microgrid system into the Swedish electricity grid. Appl Energy 2020;268:114981. https://doi.org/10.1016/j.apenergy.2020.114981.

[8] Kabus M, Nolting L, Mortimer BJ, Koj JC, Kuckshinrichs W, De Doncker RW, et al. Environmental Impacts of Charging Concepts for Battery Electric Vehicles: A Comparison of On-Board and Off-Board Charging Systems Based on a Life Cycle Assessment. Energies 2020;13:6508. https://doi.org/10.3390/en13246508.

[9] Nordelöf A, Alatalo M, Söderman ML. A scalable life cycle inventory of an automotive power electronic inverter unit—part I: design and composition. Int J Life Cycle Assess 2019;24:78–92. https://doi.org/10.1007/s11367-018-1503-3.

[10] Kumar D, Zare F, Ghosh A. DC Microgrid Technology: System Architectures, AC Grid Interfaces, Grounding Schemes, Power Quality, Communication Networks, Applications, and Standardizations Aspects. IEEE Access 2017;5:12230–56. https://doi.org/10.1109/ACCESS.2017.2705914.

[11] Qi L, Pan J, Liljestrand L, Backman M, Antoniazzi A, Raciti L, et al. DC power distribution: New opportunities and challenges. 2017 IEEE Second Int. Conf. DC Microgrids ICDCM, Nuremburg, Germany: IEEE; 2017, p. 40–6. https://doi.org/10.1109/ICDCM.2017.8001020.

[12] Planas E, Andreu J, Gárate JI, Martínez de Alegría I, Ibarra E. AC and DC technology in microgrids: A review. Renew Sustain Energy Rev 2015;43:726–49. https://doi.org/10.1016/j.rser.2014.11.067.

[13] Noritake M, Yuasa K, Takeda T, Hoshi H, Hirose K. Demonstrative research on DC microgrids for office buildings, IEEE; 2014, p. 1–5. https://doi.org/10.1109/INTLEC.2014.6972180.

[14] Sannino A, Postiglione G, Bollen MHJ. Feasibility of a DC network for commercial facilities. IEEE Trans Ind Appl 2003;39:1499–507. https://doi.org/10.1109/TIA.2003.816517.

[15] Gerber DL, Vossos V, Feng W, Marnay C, Nordman B, Brown R. A simulation-based efficiency comparison of AC and DC power distribution networks in commercial buildings. Appl Energy 2018;210:1167–87. https://doi.org/10.1016/j.apenergy.2017.05.179.

[16] Weiss R, Ott L, Boeke U. Energy efficient low-voltage DC-grids for commercial buildings, IEEE; 2015, p. 154–8. https://doi.org/10.1109/ICDCM.2015.7152030.

[17] DIN. ISO 14040:2006 - Environmental management - Life cycle assessment - Principles and framework. International Organization for Standardization; 2006.

[18] DIN. ISO 14044: Environmental Management - Life Cycle Assessment - Requirements and Guidelines. ISO; 2006.

[19] Klo W, Grahl B. Life Cycle Assessment (LCA). Wiley-VCH Verlag GmbH & Co. KGaA; 2014.

[20] Frischknecht R, Itten R, Sinha P, de Wild-Scholten M, Zhang J. Life Cycle Inventories and Life Cycle Assessments of Photovoltaic Systems. 2015.

[21] Jungbluth N, Stucki M, Flury K, Frischknecht R, Büsser S. Life Cycle Inventories of Photovoltaics. Swiss Federal Office of Energy SFOE; 2012.

[22] Verein Deutscher Ingenieure e.V. VDI 3807, Characteristic consumption values for buildings Characteristic heating-energy, electrical-energy and water consumption values – Blatt 2. Berlin, Germany: Beuth Verlag GmbH; 2014.

[23] Aebischer DB, Huser A. Energieeffizienz von Computer Netzgeräten. Zürich: Centre for Energy Policy and Economics, ETH Zürich; 2002.

[24] Andrae ASG, Andersen O. Life cycle assessment of integrated circuit packaging technologies. Int J Life Cycle Assess 2011;16:258–67. https://doi.org/10.1007/s11367-011-0260-3.
[25] Stippich A, Sewergin A, Engelmann G, Gottschlich J, Neubert M. From Ac to Dc: Demonstration of Benefits in Household Appliances, Bonn, Germany: 2017, p. 6.
[26] Waffenschmidt E, Böke U. Telecommunications Energy Conference "Smart Power and Efficiency" (INTELEC), Proceedings of 2013 35th International: date: 13-17 Oct. 2013. Piscataway, NJ: IEEE; 2013.
[27] DIN. 12464-1:2011-08: Licht und Beleuchtung – Beleuchtung von Arbeitsstätten. Deutsches Institut für Normung; 2011.
[28] Häberlin H, Kämpfer M, Zwahlen U. Neue Tests an Photovoltaik-Wechselrichtern: Gesamtübersicht über Testergebnisse und gemessene totale Wirkungsgrade. Bern Fachhochsch 2006:6.
[29] Webb V-J. Design of a 380 V/24 V DC micro-grid for residential DC distribution. University of Toledo Digital Repository, 2013.
[30] Kim H-S, Ryu M-H, Baek J-W, Jung J-H. High-Efficiency Isolated Bidirectional AC–DC Converter for a DC Distribution System. IEEE Trans Power Electron 2013;28:1642–54. https://doi.org/10.1109/TPEL.2012.2213347.
[31] Naveen T, Sekhar G. A Star-Connected Rectifier Employed by the Three-Phase Interleaved LLC Resonant Converter Used by the High-Efficiency Isolated AC–DC Converter. Int J Eng Res Appl 2015:8.
[32] De Doncker RW, Divan DM, Kheraluwala MH. A three-phase soft-switched high-power-density DC/DC converter for high-power applications. IEEE Trans Ind Appl 1991;27:63–73. https://doi.org/10.1109/28.67533.
[33] van Hoek H, Shaker Verlag GmbH. Design and Operation Considerations of Three-Phase Dual Active Bridge Converters for Low-Power Applications with Wide Voltage Ranges. 2017.
[34] Lödl M, Kerber G, Witzmann DR, Hoffmann DC, Metzger DM. Abschätzung des Photovoltaik-Potentials auf Dachflächen in Deutschland, Graz Austria: 2010, p. 14.
[35] Kasikci I, Pantenburg N. Elektroanlagen planen und projektieren. Hochsch Biberach 2008.
[36] Lucius D. Planning of Electric Power Distribution -Technical Principles. Erlangen, Germany: Siemens AG – Energy Management; 2016.
[37] Wernet G, Bauer C, Steubing B, Reinhard J, Moreno-Ruiz E, Weidema B. The ecoinvent database version 3 (part I): overview and methodology. Int J Life Cycle Assess 2016;21:1218–30. https://doi.org/10.1007/s11367-016-1087-8.
[38] IPC. IPC-2152 Designrichtlinie für die Bestimmung der Stromtragfähigkeit von Leiterplatten. 2009.
[39] Rehrmann J. Das Netzteil- und Konverter-Handbuch: Schaltungstechnik und Anwendungsgebiete von Netzteilen und Konvertern mit vielen Schaltungsbeispielen und neu entwickelten Wandlern und Netzteilen. 1. Aufl. Gudensberg: Ed. Trifolium; 2003.
[40] TDK. SMT current sense transformers EE 4.2 core 2016.
[41] DIN. DIN VDE 0100-520:2013-06 - Errichten von Niederspannungsanlagen: Teil 5-52: Auswahl und Errichtung elektrischer Betriebsmittel – Kabel- und Leitungsanlagen. Deutsches Institut für Normung; 2013.
[42] DIN. DIN EN 60228 VDE 0295:2005-09 Leiter für Kabel und isolierte Leitungen. Deutsches Institut für Normung; 2005.
[43] Horlemann Mobile Energy GmbH. Querschnittsberechnung von Kabeln und Leitungen 2018.
[44] Mersen. Bus Bar Solutions - Electrical Power Distribution 2013.
[45] Borken-Kleefeld J, Weidema BP. Global default data for freight transport per product group. Manuscript for special ecoinvent 3.0 issue of the International Journal of Life Cycle Assessment. Ecoinvent 3.0; 2013.
[46] Fraunhofer ISE. Stromerzeugung | Energy Charts 2018. https://www.energy-charts.de/energy_pie_de.htm (accessed November 8, 2018).
[47] Hecking DrH, Hintermayer M, Lencz D, Wagner J. Energiemarkt 2030 und 2050 – Der Beitrag von Gas- und Wärmeinfrastruktur zu einer effizienten CO2-Minderung. ewi Energy Research & Scenarios gGmbH; 2017.
[48] Treyer K. Market for electricity, high voltage, DE, 3.6 - Undefined, ecoinvent 3.4 (2017). Paul Scherrer Inst 2012.
[49] Treyer K. Market for electricity, low voltage, DE, 3.6 - Undefined, ecoinvent 3.4 (2017). Paul Scherrer Inst 2012.
[50] Goedkoop M, Heijungs R, Huijbregts M. ReCiPe 2008 - A life cycle impact assessment method which comprises harmonised category indicators at the midpoint and the endpoint level. 2013.
[51] Hirsch A, Parag Y, Guerrero J. Microgrids: A review of technologies, key drivers, and outstanding issues. Renew Sustain Energy Rev 2018;90:402–11. https://doi.org/10.1016/j.rser.2018.03.040.
[52] VDE Association for Electrical, Electronic and Information Technologies. German Standardization Roadmap - Low Voltage DC. Frankfurt: 2016.
[53] Häberlin DH, Zwahlen U, Kämpfer M. Neue Tests an PV-Wechselrichtern 2018:1.
[54] Infineon. Material Content Data Sheet IPP50R140CP, 2017.
[55] Lite On. Material Data Sheet GBU 1506, 2014.
[56] Taiwan Semiconductor Co,, LTD. Materials compostion declaration D2SB05, 2018.
[57] Schruter AG. Product Content Sheet Microfuse MST 250, 2014.
[58] Infineon. ColMos Power Transistor - SPW47N60CFD, 2018.

[59] Nordelöf A. A Scalable Life Cycle Inventory of an Automotive Power Electronic Inverter Unit. Chalmers University of Technology; 2017.

.

Appendix A: Parameter

Table A.1: *Range of area sizes for typical offices in m^2 and area covered by hallway depended on the total building area based on [22]*

Room type	Very Low	Low	Medium	High	Very High
Office	21	24	28	31	35
Hallway	25%	27%	30%	32%	35%

Table A.2: *Full load hours of the different considered loads based on [22]*

Type of load		Very Low	Low	Medium	High	Very High
Electrical loads	**Office, on**	1,500	1,500	1,500	1,500	1,500
$h_{fl,\,el}$	**Office, standby**	15	30	45	75	150
Overhead lighting	**Office**	678	928	1,148	1,162	1,162
	Hallway	254	312	32	320	320
Air conditioner	**Office**	426	428	452	521	594
	Hallway	71	107	122	124	125
Ventilation	**Office**	2,628	3,250	3,250	3,250	3,250
	Hallway	3,260	3,260	3,260	3,260	3,260

Table A.3: *Efficiencies of the different converters for the ac and dc microgrid systems and their differences based on Aebischer & Huser [23], Häberlin et al. [53], Stippich et al. [25] and Waffenschmidt & Böke [26]*

	Type of Microgrid System	Very Low	Low	Medium	High	Very High
PC	**ac**	**70.0%**	**74.0%**	**78.0%**	**82.0%**	**85.0%**
	dc	**73.3%**	**77.5%**	**81.7%**	**85.9%**	**89.0%**
	Difference	**4.5%**	**4.5%**	**4.5%**	**4.5%**	**4.5%**
Monitor	**ac**	**80.0%**	**82.5%**	**85.0%**	**87.5%**	**90.0%**
	dc	**82.2%**	**84.8%**	**87.4%**	**89.9%**	**92.5%**
	Difference	**2.7%**	**2.7%**	**2.7%**	**2.7%**	**2.7%**
LED	**ac**	**80.0%**	**82.5%**	**85.0%**	**87.5%**	**90.0%**
	dc	**82.2%**	**84.8%**	**87.4%**	**89.9%**	**92.5%**
	Difference	**2.7%**	**2.7%**	**2.7%**	**2.7%**	**2.7%**
Motor loads, PV system	**ac**	**80.0%**	**82.5%**	**85.0%**	**87.5%**	**90.0%**
	dc	**84.2%**	**86.8%**	**89.5%**	**92.1%**	**94.7%**
	Difference	**5.0%**	**5.0%**	**5.0%**	**5.0%**	**5.0%**
Storage system	**ac**	**80.0%**	**82.5%**	**85.0%**	**87.5%**	**90.0%**
	dc	**88.4%**	**91.2%**	**93.9%**	**96.7%**	**99.5%**
	Difference	**9.6%**	**9.5%**	**9.5%**	**9.5%**	**9.5%**
P_{dem_max}	**ac**	**100.0%**	**100.0%**	**100.0%**	**100.0%**	**100.0%**
	dc	**87.4%**	**88.5%**	**89.0%**	**90.0%**	**93.1%**
	Difference	**12.6%**	**11.5%**	**11.0%**	**10.0%**	**6.9%**

Appendix B: Materials

Table B.1: Removed components for the converter connected to the PC based on Stippich et al. (2017) [25]

Components	Material compositions and *ecoinvent* flows	Reduced Amount	Reduced Weight (g)
Heatsink	"Aluminum, wrought alloy & Section bar extrusion, aluminum", scaled according to Table 2	2	24.95
Resistor	"Resistor, metal type, THM"	2	18.57
Inductor	"Inductor, ring core choke type"	5	102.51
Capacitor	"Capacitor, film type, for THM"	2	6.48
	"Capacitor, tantalum, for THM"	3	1.63
Diode	"Diode, glass, for THM"	2	2.16
IC with board	"Printed wiring board, for SMD, unspecific"	1	3.30
MOSFET	Based on Infineon [54]	1	4.00
Bridge Rectifier	Based on Lite On [55]	1	2.03
PCB	"Printed wiring board production, for through-hole mounting, Pb free surface" scaled according to Table 2	0.007m^2	0.022
	"Mounting, through-hole technology, Pb-free solder"	0.007m^2	0.022

Table B.2: Reduced components for the converter connected to the PC based on ecoinvent dataset *power supply unit, for desktop computer* and Nordelöf et al. [9]

Components	Material compositions and *ecoinvent* flows	Total Weight (g)	Reduced Amount (%)
DC Link Capacir	"Capacitor electrolytic type < 2 cm height"	26.37	30-50
	"Capacitor electrolytic type > 2 cm height"	44.60	30-50
Casing	"Steel", scaled according to Table 2	572.00	20-40

Table B.3: Removed components for the converter connected to the monitor based on Stippich et. al. [25]

Components	Material compositions and *ecoinvent* flows	Reduced Amount	Reduced Weight (g)
Inductor	“Transformer, high voltage use”	1	9.15
Rectifying Bridge	Based on Taiwan Semiconductor Co,, LTD. [56]	1	2.10
Resistor	“Resistor, wirewound, THM”	1	0.69
Capacitor"	“Capacitor, film type, for THM”	2	4.69
	“Capacitor, for SMT”	1	0.55
Fuse	Based on Schruter AG [57]	1	0.53
PCB	“Printed wiring board production, for through-hole mounting, Pb free surface”, scaled according to Table 2	0.0017 m^2	5.24
	“Mounting, through-hole technology, Pb-free solder”	0.0017 m^2	5.24

Table B.4: Reduced components for the converter connected to the monitor based on ecoinvent dataset *power supply unit, for desktop computer* and Nordelöf et al. [9]

Components	Material compositions and *ecoinvent* flows	Total Weight (g)	Reduced Amount (%)
DC Link Capacitor	“Capacitor electrolytic type < 2 cm height”, scaled according to Table 2	6.59	30-50
	“Capacitor electrolytic type > 2 cm height”, scaled according to Table 2	11.15	30-50

Table B.5: Removed components for the converter connected to the LEDs based on Stippich et al. [25]

Components	Material compositions and *ecoinvent* flows	Reduced Amount	Scaling factor	Reduced Weight (g)
Filter and Rectifying stage	See Table B.3	1	1	0.028
Heatsink	"Aluminum, wrought alloy" scaled according to Table 2 "Section bar extrusion, aluminum", scaled according to Table 2	2	0.13	3.24
Resistor	"Resistor", metal type, THM	1	0.13	2.41
Inductor	"Inductor, ring core choke type"	5	0.13	12.17
Diode	"Diode, glass, for THM"	1	1	2.16
IC with board	"Printed wiring board, for SMD, unspecific", scaled according to Table 2	1	1	3.30
MOSFET	Based on Infineon [58]	1	1	4.00
Additional reduced PCB	"Printed wiring board production, for through-hole mounting, Pb free surface", scaled according to Table 2	0.00385m^2	0.275 * 3.08 kg/m^2	12.00
	"Mounting, through-hole technology, Pb-free solder"	0.00385m^2	0.275 * 3.08 kg/m^2	12.00

Table B.6: Reduced components for converter connected to the LEDs based on ecoinvent dataset *power supply unit, for desktop computer* and Nordelöf et al. [9]

Components	Material compositions and *ecoinvent* flows	Total Weight (g)	Reduced Amount (%)
DC Link Capacitor	"Capacitor electrolytic type < 2 cm height", scaled according to Table 2	3.43	30-50
	"Capacitor electrolytic type > 2 cm height", scaled according to Table 2	5.80	30-50
Casing	"Polyethylene production, high density, granulate", scaled according to Table 2	184.34	30-50

Table B.7: Materials used for a PCC converter based on Kim et al.[30], Naveen & Sekhar [31], Nordelöf et al. [9]

Part	***Component***	**Material compositions and *ecoinvent* flows**	**Required for 10 kW unit**
Filter	Inductor	"Inductor, ring core choke type", scaled according to Table 2	Mass: 45.36 g
VSI		Material and component composition based on Nordelöf [59], scaled internal power module according to Table 2	Amount: 1
DC Link Capacitor	At rectification side 538.2 V	Material composition for film Capacitor based on Nordelöf [59],	Mass: 132.66 g
	At microgrid side 380 V		Mass: 188.94 g
DAB	Transformer	"Copper", scaled according to Table 2	Mass: 261 g
		"Ferrit" scaled according to Table 2	Mass: 399 g
		Production and other materials according to "transformer production, high voltage use"	Mass: 0.8 * amount in dataset [g]
	PCB	"Printed wiring board production, for through-hole mounting, Pb free surface", scaled according to Table 2	Area: 579.12 m^2
		"Mounting, through-hole technology, Pb-free solder"	Area: 579.12 m^2
	MOSFETs	Materials according to Infineon [58]	Amount: 12
	Driver Board	Material and component composition based on Nordelöf [59],	Amount: 2
	Logic Board	Material and component composition based on Nordelöf [59],	Amount: 1
	Heatsink	"Aluminum, wrought alloy"	Mass: 8,996 g
		"Section bar extrusion, aluminum"	Mass: 8,996 g
Casing	Steel Casing	"Steel. Low-allowed"	Mass: 13,119 g
		"hot rolling, steel"	Mass: 13,119 g

Appendix C:

The factor S for equation (23) takes the skin and proximity effects into account. Based on Chapman and Norris (2018), the calculation has been simplified to Equation (A.1) with assuming a 3:1 width to height ratio of the cross-section area and a parameter p which is represented by Equation (A.2). The frequency (f) of the ac system is 50 Hz. The factor S is one for the dc system. This simplification is based on a single conductor, and there are additional effects to consider when connecting more conductors in parallel, depending on their layout and the gap between them. Those details are not considered in the calculations.

$$S_{ac} = \frac{0.011 * p^4}{1 + 0.19 * p^2 + 2.938 * 10^{-3} * p^4}\ ,\ S_{dc} = 1 \qquad \text{(A.1)}$$

$$\mathrm{p} \approx 1.585 * \sqrt{\frac{f}{R_{\mathrm{dc}} * 10^{-6}}} = 1.585 * \sqrt{\frac{f}{\sigma_{\mathrm{cu}} * 10^{-6} * A_{\mathrm{cs\ busbar}}}} \quad \text{(A.2)}$$